Journal of Alzheimer's Disease 23 (2011) 641–654
DOI 10.3233/JAD-2010-101389
IOS Press

Strain- and Age-related Alteration of Proteins in the Brain of SAMP8 and SAMR1 Mice

Lei Zhu[a], Jianchun Yu[b], Qiaoqiao Shi[a], Wenwen Lu[a], Bin Liu[a], Shaofeng Xu[a], Ling Wang[a], Jingxian Han[b] and Xiaoliang Wang[a,*]
[a]*Department of Pharmacology, Institute of Materia Medica, Chinese Academy of Medical Sciences & Peking Union Medical College, Beijing, China*
[b]*First Affiliated Hospital of Tianjing College of Traditional Chinese Medicine, Tianjin, China*

Handling Associate Editor: Jianzhi Wang

Accepted 13 October 2010

Abstract. In order to discover and identify the key protein biomarkers in the aging process, we performed a differential proteomic analysis of hippocampus and cortex in 5- and 15-month old senescence-accelerated mouse prone 8 (SAMP8) as well as in control strain SAM/resistant 1 (SAMR1). Using 2-DE combined with MALDI TOF/TOF mass spectrometry, about 1700 protein spots were isolated, and three groups of differentially expressed proteins were identified. The first group contained the strain-specific and non-age-related differential proteins that were differentially expressed in SAMP8 compared with SAMR1 mice. The changes might be implicated in the genetic difference between SAMP8 and SAMR1 mice; specifically, the proteins ubiquitin carboxyl-terminal esterase L3, mitofilin, adenylate kinase 4, and an unnamed protein product (gi|12847201). The proteins in the second group were age-specific, which were differentially expressed between 5- and 15-month old SAM mice. Those proteins are particularly interesting since the changes were aging-related and some of them were previously reported to be expressed in Alzheimer's disease patients. These proteins included N-myc downstream regulated gene 2, enolase 2, Cu/Zn superoxide dismutase, myosin, and two unnamed protein products (gi|74214304 and gi|74178239). The protein in the third group was SAMP8 specific-age-related protein, which was identified as heme binding protein 1. The present study provides new information about SAMP8 specific and aging-related protein changes in brain. Further investigations will be performed to reveal the significance of these proteins in brain aging process and the potential roles as biomarkers for effective diagnosis and therapy.

Keywords: Brain aging, cortex, hippocampus, proteomics, senescence-accelerated mouse

INTRODUCTION

Brain aging is associated with a decline in cognitive performance, and is the primary risk factor for Alzheimer's disease (AD) and other prevalent neurodegenerative disorders [1]. A number of neuropathological changes are observed in the aged brain, such as a reduction of brain volume, a loss of neural circuits and synaptic plasticity, as well as the formation of neurofibrillary tangles (NFT), senile plaques, and lipofuscin [2–4]. Many studies have been done for the mechanism of brain aging and several theories have been proposed, including genetic and environmental factors, DNA damage, oxidative stress, mitochondrial dysfunction, and calcium homeostasis imbalance. However, the primary cause of brain aging has not been well identified at molecular level. Correspondingly, there is

*Correspondence to: Xiaoliang Wang, Department of Pharmacology, Institute of Materia Medica, Chinese Academy of Medical Sciences & Peking Union Medical College, 1. Xiannongtan Street, Beijing 100050, China. Tel.: +86 106 316 5330; Fax: +86 106 301 7757; E-mail: wangxl@imm.ac.cn.

ISSN 1387-2877/11/$27.50

no "biomarker" for accurate and effective diagnosis at its insidious onset [3, 5, 6]. Clues may come from the animal models.

The senescence-accelerated mouse (SAM) is an accelerated aging mouse model that was established through phenotypic selection from a common genetic pool of AKR/J strain of mice [7]. It contains nine senescence-accelerated mouse prone (SAMP) substrains and three senescence-accelerated mouse resistant (SAMR) substrains, each of which exhibits characteristic disorders. Among its prone substrains, SAM/prone 8 (SAMP8) exhibits a more accelerated senescence process and has a shortened liftspan, ranging from 10 months to 17 months, as compared with SAM/resistant 1 (SAMR1) mice, which show normal aging process and are usually used as controls [8]. Behavioral studies showed that learning and memory deficits started as early as 6 months and worsened with aging in SAMP8 mice [9, 10]. Mitochondrial dysfunction, increased oxidative stress, and tau hyperphosphorylation were also observed at an early age in the brain of SAMP8 mice [11, 12]. In addition, SAMP8 mice showed an age-related increase in mRNA and protein levels of amyloid-β protein precursor (AβPP). The amyloid-β (Aβ) was significantly increased at 9 months and the amyloid plaques formation in about 16 months were also observed in SAMP8 [13, 14]. Therefore, SAMP8 is a useful animal model to investigate aging [15]. Because mitochondrial function, tau phosphorylation, and Aβ accumulation are difficult to be measured in patients and animals, new biomarkers are needed for diagnosis and treatment of age-related diseases such as AD.

Two-dimensional gel electrophoresis (2-DE) based proteomic analysis is a direct and systematic tool to discover proteins which undergo changes in expression level and may underlie the differences of phenotypes. Moreover, it can resolve distinct isoforms of protein and identify post-translational modifications which might be functionally important [16]. Several proteomic studies of SAMP8 brain tissue have been reported, including comparative analysis between 4- and 12-month old SAMP8 mice [17], as well as 6-month old SAMP8 versus age-matched SAMR1 mice [18]. Despite those studies, it was still difficult to reveal strain- or aging-dependent protein changes. It is known that SAMP8 mice are presymptomatic at 5 months and are symptomatic at about 15 months with obvious and typical neurodegenerative characteristics of aging [10, 15]. Therefore, we performed the proteomic analysis of hippocampus and cortex, the most relevant brain regions for learning and memory, in SAMP8 and SAMR1 mice at presymptomatic (5-month old) and symptomatic (15-month old) stages. The protein expression differences were compared not only between SAMP8 and SAMR1 strain at the same age, but also between 5- and 15-month old mice in both strains to investigate the brain protein alterations during aging.

MATERIALS AND METHODS

Animals and sample preparation

5- and 15-month old male SAMP8 and SAMR1 mice were supplied from the First Affiliated Hospital of Tianjing College of Traditional Chinese Medicine, China. We used five mice per age group of both strains. After mice were sacrificed, the total hippocampus and total cortex tissues were removed immediately and stored in liquid nitrogen until use. All experiments were performed according to the guidelines of the Chinese Academy of Medical Science for Institutional Animal Care, based on the National Institute of Health Guide for the care and use of laboratory animals. Each hippocampus or cortex sample was separately homogenized in a lysis buffer [7 M urea, 2 M thiourea, 4% CHAPS, 1% dithiothreitol (DTT), 0.5% IPG buffer (pH 3–10 NL, GE Healthcare), and 1% Protease Inhibitor Mix (Roche)]. Then the samples were centrifuged at $1{,}000 \times g$ at 4°C for 10 min to remove debris, the supernatant was further centrifuged at $12{,}000 \times g$ at 4°C for 10 min. Then the supernatant was collected and stored at –80°C until use. Protein content was determined by a 2-D Quant Kit (GE Healthcare). And separate proteomic assays were performed for hippocampus and cortex.

2-DE analysis

Individual 2-DE gel of single sample from one mouse was run. The first dimension was performed on Ettan IPGphor II IEF system (GE Healthcare). 350 μl rehydration buffer [8 M urea, 2% CHAPS, 0.5% IPG buffer (pH 3–10 NL), 1% Destreak reagent (GE Healthcare), and 0.002% bromphenol blue] containing 120 μg protein (for the comparative analysis of protein spots) or 1 mg protein (for mass spectrometry of protein identification) were loaded onto nonlinear IPG strips (18 cm, pH 3–10 NL, GE Healthcare). The isoelectric focusing was performed at 50 V for 12 h linearly; 200 V for 1 h linearly; 500 V for 1 h linearly, 1000 V for 1 h linearly; 8000 V for 1 h rapidly; and

finally achieved 70,000 Vh at the voltage of 8000 V. The strips were then equilibrated for 15 min in equilibration buffer containing 6 M urea, 0.05 M Tris-Cl (pH 8.8), 2% sodium dodecyl sulfate (SDS), 30% glycerol, and 1% DTT, and re-equilibrated for 15 min in the same buffer containing 2.5% iodoacetamide in place of DTT. The equilibrated gel strip was placed on the top of a 12.5% SDS-polyacrylamide gel electrophoresis (PAGE) gel, and embed with 0.5% low-melt agarose (Sigma). Then the second dimension separation was performed in an Ettan DALTsix Electrophoresis System (GE Healthcare) at 16°C as follows: 2.5 W/gel constant powers for 45 min, and then 17 W/gel constant powers until the bromophenol blue front reached the bottom of the gels.

Gel staining and image analysis

After performing 2-DE, the analytic gels were silver stained using PlusOne Silver Staining Kit (GE Healthcare). And the preparative gels were stained by "blue-silver" method as described previously [19]. The silver stained gels were scanned and saved in TIFF format using Umax Power look 2100XL scanner (Umax, Taiwan, China). Image analysis was carried out by using ImageMaster 2D Platinum software (GE Healthcare). Concretely, the protein spot in the gel was detected, and its abundance was quantified as a normalized volume based on its optical density and area. The normalized volume of each spot from five individual gels from the two cohorts was compared between different groups using Student's *t*-test. Variation ratio of protein spot volumes between two different groups was calculated by using ImageMaster 2D Platinum software. "Ratio = 1000000, 10^6" represented the characteristic that the spot did not exist in one cohort, that was the difference of "all" or "none". "+" and "–" was placed before the value of variation ratio represented "up-regulation" and "down-regulation", respectively. Only spots with p values <0.05 and $\geq$2-fold variation ratio were considered as changed and subjected to trypsin digestion.

In-gel tryptic digestion of proteins

Above differentially expressed protein spots were excised from the "blue-silver" stained gels, and sliced into small cubes. The gel slices were destained in microtubes with 40% acetonitrile (ACN)/100 mM NH_4HCO_3 and dried completely by centrifugal lyophilization. For digestion, the dried gel slices were swollen in 20 μl of 25 mM NH_4HCO_3 (pH 8.0) containing 100 ng trypsin (Sigma). After 30 min incubation on ice, 20 μl of 25 mM NH_4HCO_3 was supplemented to keep the gel pieces wet and the enzymatic digestion continued for 16 h at 37°C. The typical peptides were extracted by two steps. First, the gel pieces were incubated with 100 μl of 5% trifluoroacetic acid (TFA) for 30 min in 40°C water bath, followed by sonication for 3 min, and then incubated for another 30 min. The second extraction step was the same with the first step besides replacing 5% TFA with 50% ACN/2.5% TFA, and the temperature of water bath was set at 30°C. The two extraction solutions were pooled, lyophilized and re-dissolved in 0.1% TFA.

Matrix-assisted laser desorption ionization time-of-flight/time-of-flight mass spectrometry (MALDI TOF/TOF MS)

The matrix material α-cyano-4-hydroxy-cinnamic acid (α-CCA, sigma) was dissolved in 50% ACN/0.1% TFA at a concentration of 5 mg/ml. Then the α-CCA solution and the extracted peptides were mixed in a 1 : 1 ratio. 1 μl of the mixture was deposited onto the MALDI target plate and allowed to dry at ambient temperature. Measurements were performed on a 4800 MALDI TOF/TOF (Applied Biosystems, USA), operated in reflector mode. Monoisotopic peptide mass was assigned and used for database searching. Peptide mass fingerprinting (PMF) was carried out on all known protein entries from the species of Mus musculus in the NCBI nr protein database using the MASCOT search engine (Matrix Science, UK) for protein identification. Up to one missed cleavage per peptide was allowed, a mass tolerance of 50 ppm was used and some variable modifications were taken into account, such as carbamidomethylation for cysteine and oxidation for methionine. In some cases, MS/MS on selected precursor ions was performed to add additional confidence to the PMF search results. And the MS/MS search parameters were also assumed to be monoisotopic, carbamidomethylation at cysteine residues and oxidation at methionine residues. A 0.3 Da MS/MS mass tolerance was used for searching. A probability-based MOWSE scores were estimated by comparison of search results against estimated random match population and were reported as $-10 \times \log 10\ (P)$, where P is the probability that the identification of the protein is a random event. Protein identification was repeated twice using spots from different gels and considered significant if the MASCOT score was higher than the probability p value <0.05 for a random match.

RESULTS

Protein spots changed in the hippocampus and cortex of SAMP8 versus SAMR1 mice

Reproducible high-resolution 2-DE maps were constructed for hippocampal and cortical proteins of SAMP8 and SAMR1 mice, respectively. Each group contained five individual 2-DE gels. For each gel, more than 1,700 spots were visualized by silver-stained and detected using ImageMaster 2D Platinum software. The representative 2-DE separation profile was shown in Fig. 1.

In order to reveal the proteins changed specifically in SAMP8 mice, the differential expression of protein spots in the hippocampus and cortex was compared between SAMP8 and age-matched SAMR1 mice. In the hippocampus of 5-month old SAMP8, 12 protein spots were found differentially expressed in comparison with SAMR1 mice. Among them, 1 protein (spot 1481) was upregulated (its variation ratio was more than +2), 2 proteins (spots 173a and 293) disappeared (their variation ratios were -10^6), 4 proteins (spots 173b, 173c, 1144a, and 1404) were down-regulated (their variation ratios were less than –2), and 5 proteins (spots 173d, 316, 915, 1144b, and 1475) presented only in SAMP8 mice (their variation ratios were $+10^6$). In the cortex of SAMP8 mice, these 12 spots were also differentially expressed in the same manner as in the hippocampus. The detailed variation ratios of these differential protein spots were summarized in Table 1.

At 15 months of age, 13 differential spots were found in SAMP8 compared with SAMR1 mice, which contained above mentioned 12 differential spots. The 12 spots were not assigned as significant differences with age (between 5 and 15 months old), indicating that they changed in a strain-specific manner and could be implicated in the genetic difference between SAMP8 and SAMR1 mice. One additional spot (spot 2379) was found to be down-regulated only in the hippocampus of 15-month old SAMP8, which showed no statistical differences in the cortex. And its expression level was significantly decreased with age in SAMP8 mice, but not in SAMR1 mice. The data suggested that spot 2379 changed in both strain- and age-specific manner. The expanded hippocampal images of these differential spots were shown in Fig. 2. (Cortical images were not shown.) Above data suggested that the differential expressions were mostly SAMP8 specific.

Protein spots changed with age in both strains of SAM mice

In order to reveal the proteins changed in age-dependent manner, differential analysis of hippocampus and cortex protein profiles was performed between 5- and 15-month old SAM mice. Eight differential protein spots were found in both tissues of 15-month old SAM mice compared to 5-month old mice. The 2-DE gel cortical images of these differential spots were shown in Fig. 3. (Hippocampus images were not shown.) Our results showed that spots 1333 and 2440 were increased in both tissues of SAMP8

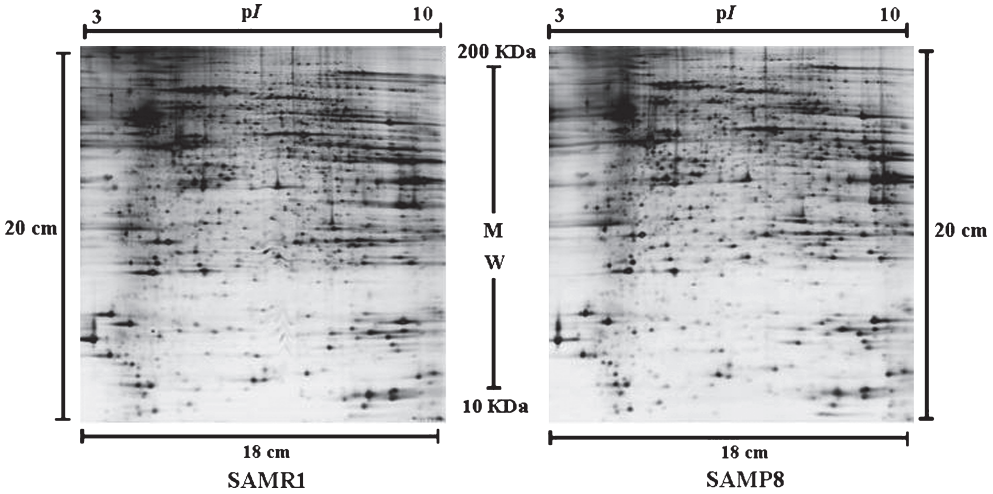

Fig. 1. Representative silver-stained 2-DE gels of hippocampus proteins from 15-month old SAMP8 and SAMR1 mice. About 120 μg protein was applied on an IPG strip (18 cm, pH 3–10 NL), followed by a 12.5% SDS-PAGE gel. For each gel, more than 1,700 spots were visualized by silver-stained and detected using ImageMaster 2D Platinum software.

Table 1
Variation ratios of the protein spots differentially expressed in SAMP8 versus SAMR1 mice

	Spot no.:	173a	173b	173c	173d	293	316	915	1144a	1144b	1404	1475	1481	2379
Changed at 5 months	Hippocampus	-10^6	–2.14	–2.32	$+10^6$	-10^6	$+10^6$	$+10^6$	–3.61	$+10^6$	–2.09	$+10^6$	+10.98	/
	Cortex	-10^6	–2.01	–2.01	$+10^6$	-10^6	$+10^6$	$+10^6$	–3.61	$+10^6$	–2.35	$+10^6$	+9.28	/
Changed at 15 months	Hippocampus	-10^6	–2.45	–2.36	$+10^6$	-10^6	$+10^6$	$+10^6$	–4.58	$+10^6$	–2.19	$+10^6$	+9.45	–2.04
	Cortex	-10^6	–2.22	–2.43	$+10^6$	-10^6	$+10^6$	$+10^6$	–5.49	$+10^6$	–2.10	$+10^6$	+9.37	/

The hippocampal and cortical proteome of SAMP8 were compared with age-matched SAMR1 mice by ImageMaster 2D Platinum software. Concretely, the protein spot in the gel was detected, and its abundance was quantified as a normalized volume based on its optical density and area. The normalized volume of each spot from five individual gels from the two cohorts was compared between different groups using Student's *t*-test. Variation ratio of protein spot volumes between two different groups was calculated by ImageMaster 2D Platinum software. Spots with p values <0.05 and $\geq$2-fold variation ratio between groups were considered as the differential spots. p values of the differential spots in this table were all less than 0.05, and their variation ratio were more than 2 as they were shown. "Ratio = $+10^6$" meant the spot presented only in SAMP8 mice, and "Ratio = -10^6" meant the spot disappeared in SAMP8 as compared with SAMR1 mice. "+" and "–" before the value of variation ratio represented "up-regulation" and "down-regulation" of the differential protein in SAMP8 compared with the age-matched SAMR1 mice, respectively. The data were defined by ImageMaster 2D Platinum software.

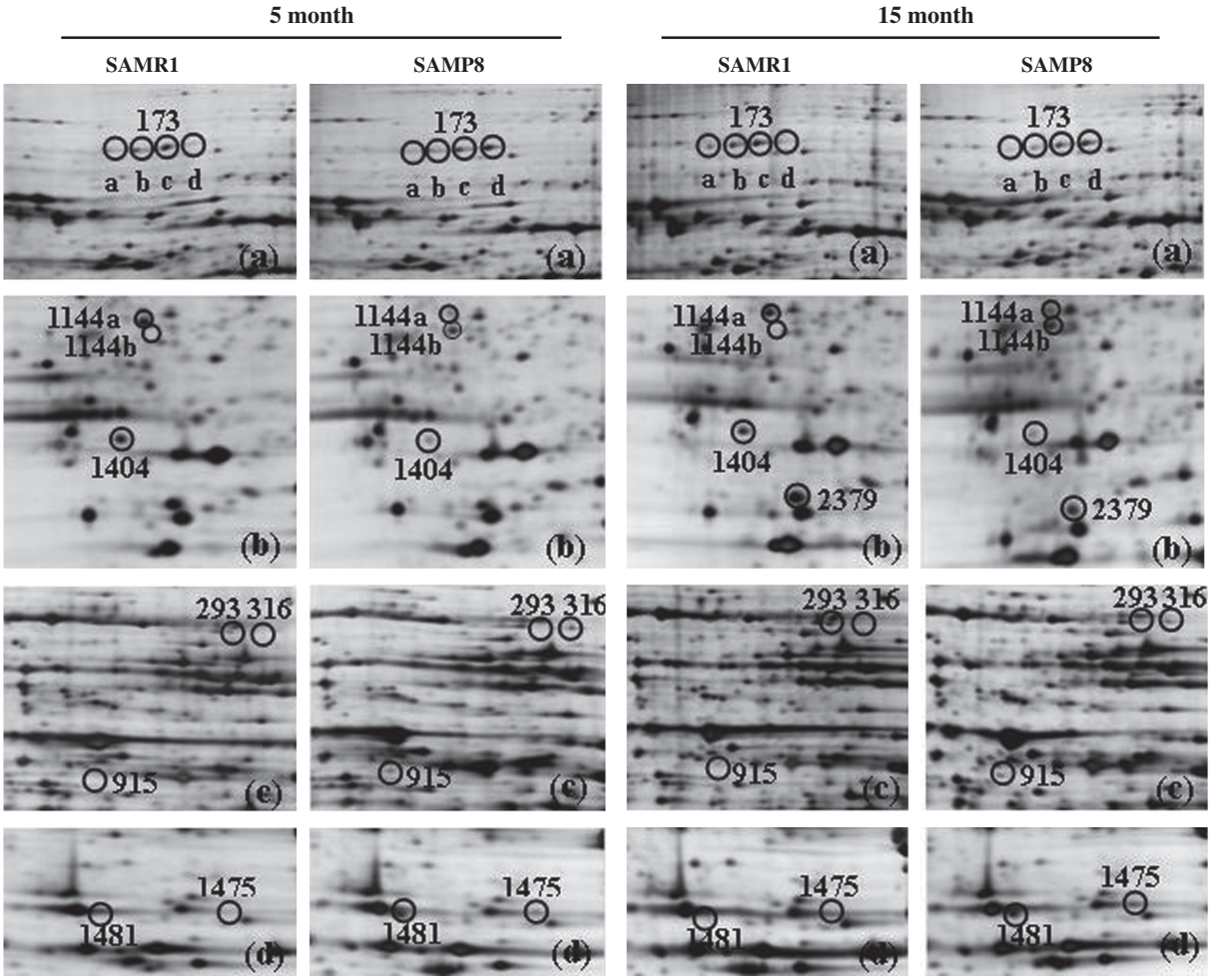

Fig. 2. Expanded hippocampal images of protein spots differentially expressed in SAMP8 versus SAMR1 mice. The differential expression of protein spots in the hippocampus and cortex was compared between SAMP8 and age-matched SAMR1 mice at 5 and 15 months old. The differentially expressed spots in the hippocampus were marked with black circles. (Cortical images were not shown.) Their variation ratio and detailed identification information were shown in Tables 1 and 3, respectively.

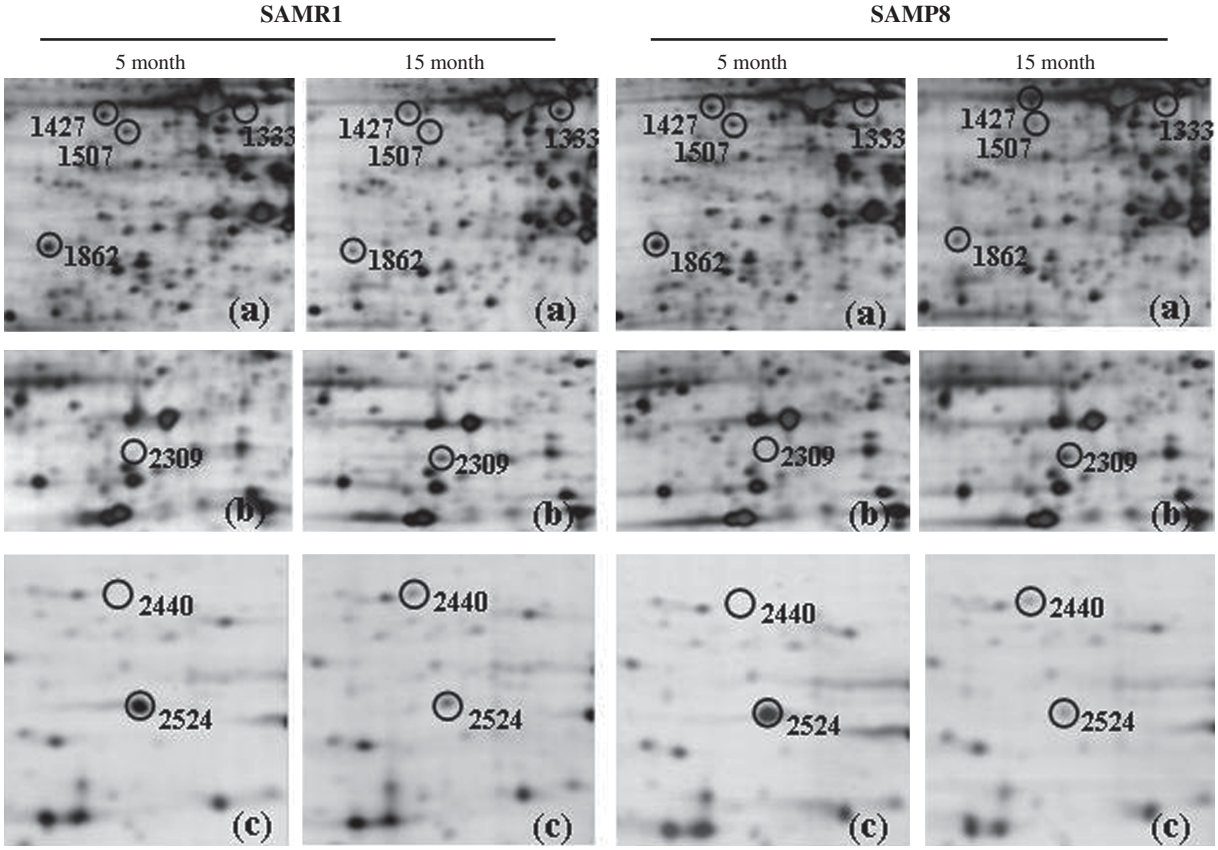

Fig. 3. Expanded cortical images of protein spots differentially expressed at 15 months old versus 5 months old SAM mice. The differential expression of protein spots in the hippocampus and cortex was compared between the ages of 5- and 15-month old SAM mice. The differentially expressed spots in the cortex were marked with black circles. (Hippocampal images were not shown.) Their variation ratio and detailed identification information were shown in Tables 2 and 4, respectively.

Table 2
Variation ratios of the protein spots differentially expressed at 15 months old versus 5 months old in SAM mice

	Spot no.:	1333	1427	1507	1862	2309	2379	2440	2524
Changed in SAMP8	Hippocampus	+2.11	/	/	/	/	–2.05	+2.09	–2.02
	Cortex	+2.09	–2.27	–2.24	–2.32	+2.18	/	+2.77	–2.71
Changed in SAMR1	Hippocampus	+2.98	/	/	/	/	/	+3.88	–3.78
	Cortex	+2.45	–2.20	–2.05	–2.31	+2.16	/	+2.98	–4.14

Comparative proteomics were carried out between 5- and 15-month old mice within the same strain by using ImageMaster 2D Platinum software. Spots with p values <0.05 and ≥2-fold variation ratio between groups were considered as differential spots. p values of the differential spots in this table were all less than 0.05, and their variation ratio were more than 2 as they were shown. "+" and "–" before the value of variation ratio represented the "up-regulation" and "down-regulation" of the differential protein in 15-month old mice compared with 5-month old mice. The data were defined by ImageMaster 2D Platinum software.

and SAMR1 mice (their variation ratios were more than +2). Spot 2524 was decreased in the hippocampus and cortex in both strain of mice (the variation ratios were less than –2). Spots 1427, 1507, and 1862 were specifically decreased in the cortex of both mice (their variation ratios were less than –2). By contrast, spot 2309 was significantly increased in the cortex of both mice (the variation ratios were more than +2). Spot 2379 was specifically decreased in the hippocampus of 15 month old SAMP8 mice (the variation ratio was less than –2). None of the variation ratios of the age-dependent differential protein spots were "$+10^6$" or "-10^6". The detailed values were summarized in Table 2. It was interesting that these protein alterations were tissue instead of stain specific, except spot 2379.

None of these protein spots (except spot 2379) was shown as significant differences between SAMP8 and SAMR1 mice at the both ages. Therefore, these differentially expressed proteins were considered to be related to age rather to strain, and might be associated with brain aging process.

Identification of differential proteins

To identify the differential proteins, the above-mentioned spots were excised for in-gel trypsin proteolysis and subsequently identified by PMF analysis combined with MS/MS results. The identification was repeated twice using spots from different gels. Among 13 specifically changed spots in SAMP8 mice, 4 spots (spots 293, 316, 915, and 1475) were very faint and could not be identified unambiguously by MS. The remaining 9 spots obtained clear MS data and were identified by Mascot searches in the NCBI nr database: they were mitochondrial inner membrane protein (also termed mitofilin, spots 173a, 173b, 173c, and 173d), ubiquitin carboxyl-terminal esterase L3 (Uchl3, spot 1404), adenylate kinase 4 (AK4, spot 1481), heme binding protein 1 (spot 2379), and an unnamed protein product with GI accession number of gi|12847201 (spots 1144a and 1144b). For the other group of proteins (8 spots) which were differentially expressed with age in both mouse strains, except spot 2440, 7 spots were successfully identified as N-myc downstream regulated gene 2 (NDRG2, spot 1333), enolase 2 (spot 1507), myosin, light polypeptide 3 (spot 2309), Cu/Zn superoxide dismutase (Cu/Zn SOD, spot 2524), heme binding protein 1 (spot 2379), and two unnamed protein products with GI accession number of gi|74214304 (spot 1427) and gi|74178239 (spot 1862). All protein identifications are consistent with the expected MW and isoelectric point (p*I*) range based on their positions on the gel. The trypsin peptide MS spectrums of these identified proteins were shown in Figs 4, 5, and their detailed information was listed in Tables 3 and 4.

2-DE map allowed the high resolution of slight charge differences. Mitofilin was observed as 4 distinct protein spots (spots 173a, 173b, 173c, and 173d) with almost the same MW but slightly different p*I,* presumably representing protein modification. In the hippocampus and cortex of SAMR1 mice, mitofilin existed as 3 more acidic forms (spots 173a, 173b, and 173c). However, the most acidic form (spot 173a) disappeared, and a more alkaline form (spot 173d) freshly appeared in SAMP8 mice compared with SAMR1 mice. Based on the present mass spectral data, the causes for this alkaline isoelectric shift of mitofilin in SAMP8 mice could not yet be ascertained.

In addition to the isoelectric changes, another interesting phenomenon was also found. That is, protein spots 1144a and 1144b were both identified as an unnamed protein product with GI accession number of gi|12847201. By comparison of their mass spectral profiles, we found that spot 1144a represented the full-length form of this unnamed protein product. However, the tryptic fragment of spot 1144a contained 46 amino acids at the amino-terminal, which was missing from the mass spectra of spot 1144b (Fig. 5). The full-length form (spot 1144a) of this unnamed protein product was significantly decreased in the hippocampus and cortex of SAMP8 compared with the age-matched SAMR1 mice. Meanwhile, the amino-terminal truncated form (spot 1144b) only presented in SAMP8 mice, indicating the protein modified from full length form to short form in SAMP8 mice.

DISCUSSION

In the present study, we performed a differential proteomic analysis of hippocampus and cortex in SAMP8 and its reference strain SAMR1 mice at the ages of 5 and 15 month. Three groups of differentially expressed proteins were found and identified (Table 5).

The first group contained strain-specific differential proteins, which included 12 protein spots expressed differentially in the hippocampus and cortex of both 5- and 15-month old SAMP8 in comparison with age-matched SAMR1 mice. For these 12 differential proteins, there were no significant differences with age (between 5 and 15 months old), indicating that they might be involved in the genetic difference between SAMP8 and SAMR1 mice instead of aging-related changes. Except 4 faint spots (spots 293, 316, 915, and 1474), the remaining 8 spots were identified as Uchl3, 4 isoforms of mitofilin, AK4, and an unnamed protein product (gi|12847201) with two isomers.

The second group of differentially expressed proteins changed in an age-specific manner. There were 7 protein spots in this group, differentially expressed with age (between 5 and 15 month) in both strains, and none of them was shown significant differences between SAMP8 and SAMR1 mice. Therefore, they were considered to be related to age rather than strain, and might be associated with brain aging process. Except one faint spot (spot 2440), the other 6 spots were identified as NDRG2, enolase 2, Cu/Zn SOD, myosin

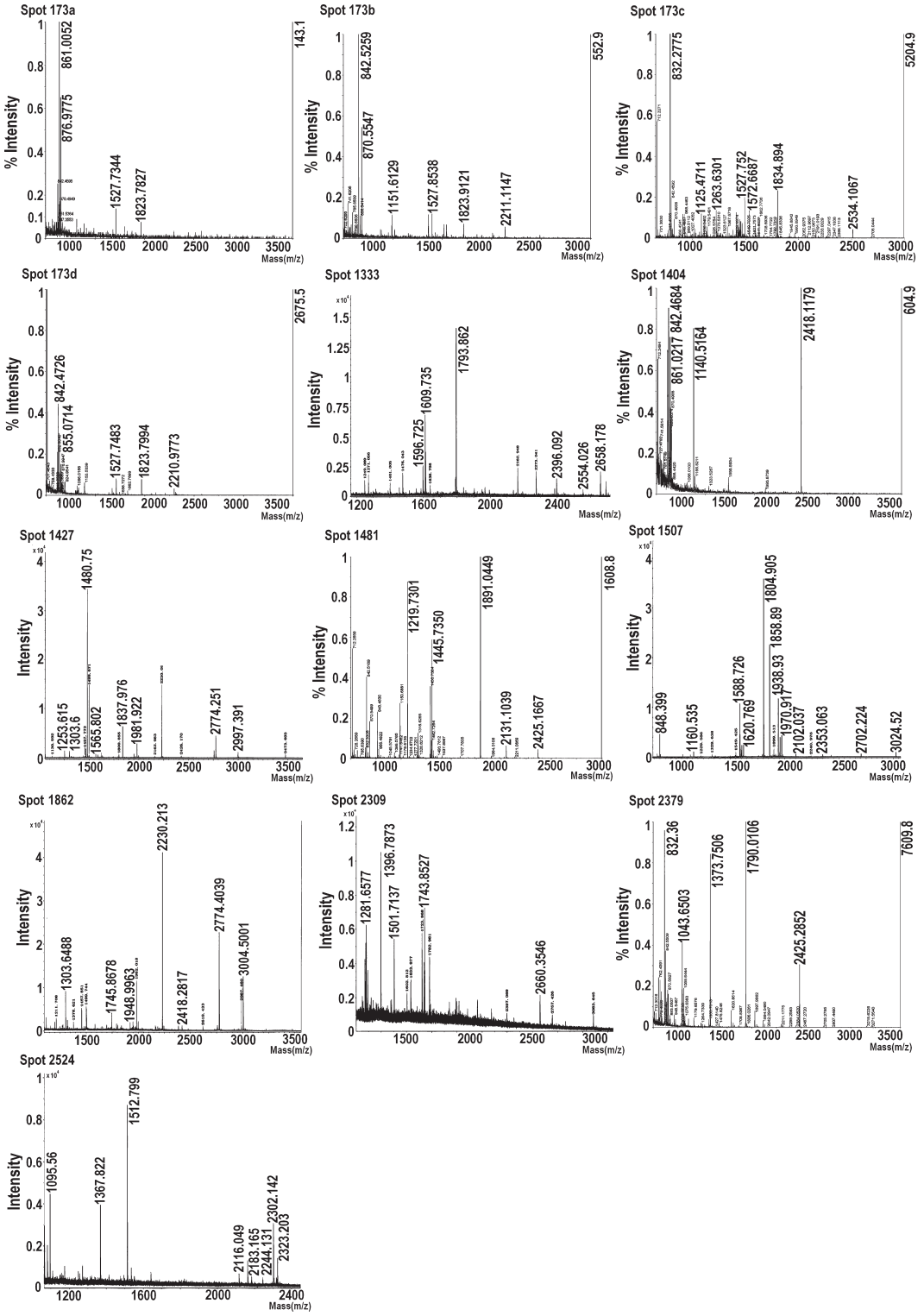

Fig. 4. MALDI TOF mass spectra of the tryptic digests of the differential protein spots. The differential spots were excised from 2-DE gels for in-gel tryptic digestion and identified by combining PMF and MS/MS results. The PMF spectrums were shown. The x-axis represented mass-to-charge ratio (m/z), and the y-axis represented relative abundance. The peptide masses were labeled and annotated with corresponding m/z.

A **Spot 1144a:**

MEGEGGEATE QPGLNGAAAA AAAEAPDETA QALGSADDEL SAKLLRRADL
NQGIGEPQSP SRRVFNPYTE FKEFSRKQIK DMEKMFKQYD AGRDGFIDLM
ELKLMMEKLG APQTHLGLKS MIQEVDEDFD SKLSFREFLL IFRKAAAGEL
QEDSGLHVLA RLSEIDVSTE GVKGAKNFFE AKVQAINVSS RFEEEIKAEQ
EERKKQAEEV KQRKAAFKEL QSTFK

Spot 1144b:

MEGEGGEATE QPGLNGAAAA AAAEAPDETA QALGSADDEL SAKLLRRADL
NQGIGEPQSP SRRVFNPYTE FKEFSRKQIK DMEKMFKQYD AGRDGFIDLM
ELKLMMEKLG APQTHLGLKS MIQEVDEDFD SKLSFREFLL IFRKAAAGEL
QEDSGLHVLA RLSEIDVSTE GVKGAKNFFE AKVQAINVSS RFEEEIKAEQ
EERKKQAEEV KQRKAAFKEL QSTFK

B

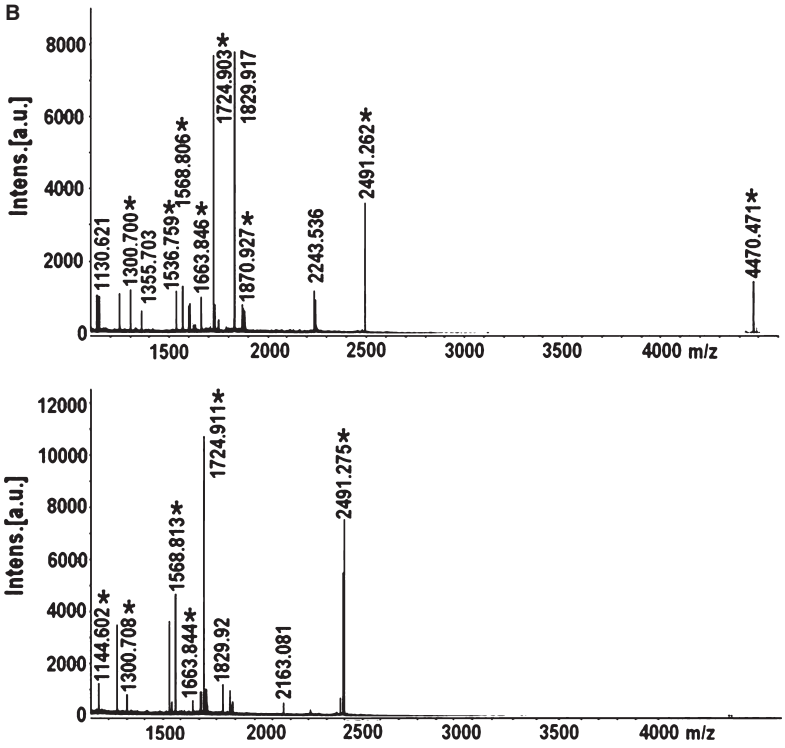

Fig. 5. MALDI TOF mass spectral analyses of tryptic digests of protein spots 1144a and 1144b. A, coverage map, with underlined residues indicating peptides detected by PMF. B, MALDI TOF PMF spectrum of the tryptic digests of spot 1144a (upper spectrum) and spot 1144b (lower spectrum). *Represented peptides that matched the theoretically predicted peptide masses in unnamed protein product with GI accession number of gi|12847201. Note that the ion at m/z 4470.471 in the upper spectrum (spot 1144a) representing the amino-terminal 46 amino acids was missing from the lower spectrum (spot 1144b).

and two unnamed protein products (gi|74214304 and gi|74178239).

The third group of differentially expressed proteins was both strain- and age-relevant, which contained one protein spot and was identified as heme binding protein 1. This differential protein was found down-regulated in the hippocampus of 15-month old SAMP8 in comparison with age-matched SAMR1 mice, and was also decreased with age in SAMP8 strain but not in SAMR1 strain. It indicated that heme binding protein 1 might be mainly associated with pathologically accelerated aging of SAMP8 mice.

For the first group of differentially expressed proteins, the alteration of Uchl3, mitofilin, and AK4 have been previously reported in SAMP8 mice. Concretely, the differential expression of Uchl3 and mitofilin was found in the hippocampus of 6-month old SAMP8 compared with the age-matched SAMR1 mice by

Table 3
Identification data of proteins significantly altered in SAMP8 compared with the age-matched SAMR1 mice

Spot no.	Protein name	Accession GI no. NCBI	Sequence coverage (%)	p*I*, MW	MOWSE score*	Changed in SAMP8 vs. SAMR1
173a	Mitochondrial inner membrane protein (Mitofilin)	29427692	2	6.18, 83848.2	65	
173b	Mitochondrial inner membrane protein (Mitofilin)	29427692	16	6.18, 83848.2	84	
173c	Mitochondrial inner membrance protein (Mitofilin)	29427692	24	6.18, 83848.2	155	Consistent alkaline shift of p*I*
173d	Mitochondrial inner membranee protein (Mitofilin)	29427692	12	6.18, 83848.2	189	
293	Cannot be identified					
316	Cannot be identified					
915	Cannot be identified					
1144a	Unnamed protein product	12847201	33	5.07, 26783.6	368	Full-length form
1144b	Unnamed protein product	12847201	36	5.07, 26783.6	269	Amino-terminally truncated form
1404	Ubiqutin carboxyl-terminal esterase L3 (Ubiqutin thiolesterase)	28913414	23	4.96, 26135	146	Down-regulated
1475	Cannot be identified					
1481	Adenylate kinase 4	55991512	36	7.02, 25046.1	251	Up-regulated
2379	Heme binding protein 1	15215071	56	5.18, 21039.3	495	Down-regulated

*MOWSE scores are determined using the search engine Mascot. This program uses a probability-based MOWSE scoring program to determine significant peptide matches. Scores are reported as $-10 \times \log10\,(P)$, where P is the probability that the observed match is a random event. For this data set, protein scores greater than 60 is considered significantly ($p < 0.05$). Scores listed are significant matches. All identified proteins agree with the expected MW and p*I* range based on their positions on the gel.

Table 4
Identification data of proteins significantly changed with age in both strains of SAM mice

Spot no.	Protein name	Accession GI no. NCBI	Sequence coverage (%)	p*I*, MW	MOWSE score*	Changed at 15 months old vs. 5 months old
1333	N-myc downstream regulated gene 2, isoform CRA_b	148710328	32	4.91, 32600	82	Up-regulated
1427	Unnamed protein product	74214304	31	5.17, 56662	68	Down-regulated
1507	Enolase 2, gamma neuronal	7305027	48	4.99, 47267	168	Down-regulated
1862	Unnamed protein product	74178239	29	4.94, 27392	82	Down-regulated
2309	Myosin, light polypeptide 3, isoform CRA_a	148677054	28	5.03, 24241	68	Up-regulated
2379	Heme binding protein 1	15215071	56	5.18, 21039.3	495	Down-regulated
2440	Cannot be identified					
2524	Cu/Zn superoxide dismutase	226471	56	6.03, 15752	158	Down-regulated

*MOWSE scores are determined using the search engine Mascot. This program uses a probability-based MOWSE scoring program to determine significant peptide matches. Scores are reported as $-10 \times \log10\,(P)$, where P is the probability that the observed match is a random event. For this data set, protein scores greater than 64 is considered significantly ($p < 0.05$). Scores listed are significant matches. All identified proteins are consistent with the expected MW and p*I* range based on their positions on the gel.

a proteomic analysis [18]. And a recent proteomic study of astrocyte cultures showed that AK4 was significantly increased in astrocytes from SAMP8 in comparison with SAMR1 mice [20]. The alterations of these proteins were not found in SAMR1 or samples from human during aging process. The authors just showed the differences of those proteins between SAMP8 and SAMR1 at the same age. Our study further compared them at the different ages and demonstrated that these proteins were not age-related, and they might be genetically specific changes in SAMP8 mice. The importance of above 3 proteins for aging process is not clear until now. Uchl3 is an important deubiquitinating enzyme, which is vital to degrade and remove damaged and misfolded proteins [21]. The down-regulation of Uchl3 in SAMP8 mice could result in aggregation of aberrant proteins which is toxic to neurons and might induce the accelerative aging process in SAMP8 strain. Mitofilin and AK4 are both mitochondrial proteins. Mitofilin exists in the mitochondrial intermembrane space, and is indispensable for sustaining normal mitochondrial morphology and function [22]. In the present study, it was found to exist in four isomers with a consistent shift of p*I*. Especially, one

Table 5
Categorization of the differentially expressed proteins in the brains of SAM mice

Category	Differential proteins	Reported in SAMP8	Reported in AD	Not reported previously	References
Strain-specific proteins	Uchl3	Yes			[18]
	Mitofilin	Yes			[18]
	AK4	Yes			[20]
	Unnamed protein product (gi|12847201)			Yes	/
	Unidentified protein spots (spots 293, 316, 915, 1475)			Yes	/
Age-specific proteins	NDRG2		Yes		[26]
	Enolase 2		Yes		[30–32]
	Cu/Zn SOD	Yes	Yes		[11, 34, 35]
	Myosin			Yes	/
	Unnamed protein product (gi|74214304)			Yes	/
	Unnamed protein product (gi|74178239)			Yes	/
	Unidentified protein spots (spot 2440)			Yes	/
Strain- and age-specific protein	Heme binding protein 1			Yes	/

Three groups of differentially expressed proteins were found and identified in the proteomic analysis of 5- and 15-month old SAMP8 and its control strain SAMR1 mice in the present study. The first group included the strain-specific differential proteins that were differentially expressed in SAMP8 compared with SAMR1 mice. Among them, the alteration of Uchl3, mitofilin, and AK4 in SAMP8 mice were previously reported; the unnamed protein product (gi|12847201) was found to be implicated in brain aging for the first time; and spots 293, 316, 915, 1475 were not identified successfully. The second group included the age-specific differential proteins that were differentially expressed between 5- and 15-month old SAM mice. They might be associated with brain aging. Among these proteins, NDRG2, enolase 2 and Cu/Zn SOD were already known to be implicated in AD and neurodegeneration; myosin and two unnamed protein products (gi|74214304 and gi|74178239) were never reported to be implicated in brain aging; and spot 2440 was not identified successfully. The protein in the third group was both strain- and age-specific and was identified as heme binding protein 1, which was reported to be related to brain aging for the first time.

isomer (173a) disappeared and one (173d) uniquely appeared in SAMP8, which might have been due to the specific modification of this protein in SAMP8 mice. This change might contribute to the mitochondrial dysfunction in SAMP8 mice and remains to be elucidated. AK4 is a phosphotransferase that catalyzes the interconversion of adenine nucleotides [23] and was recently reported as a stress responsive protein that could protect cells from oxidative stress [24]. We found AK4 was significantly increased in the hippocampus and cortex of both 5- and 15-month old SAMP8 compared with SAMR1 mice, which might be a compensation for the oxidative stress in SAMP8 mice.

The unnamed protein product (gi|12847201) found in our study has never been reported as a brain protein. We performed database searching (http://hits.isb-sib.ch/cgi-bin/PFSCAN) and tried to explore its possible role in brain aging. This protein product (gi|12847201) putatively contains four myristylation sites which are involved in lipid modifications and play roles in association of proteins in lipid rafts [25], and two EF-hand domains refer to Ca^{2+}-binding activity. These features could indicate the involvement of this protein in Ca^{2+} signaling. This novel potential signaling protein existed as two forms in the present study: spot 1144a existed as the full-length form and was significantly decreased in SAMP8 compared with the age-matched SAMR1 mice; spot 1144b only presented in SAMP8 mice which shown amino-terminally truncated form, it could be resulted from proteolytic degradation in SAMP8 mice. Since alterations in calcium homeostasis are proposed to play a central role in the process of neuronal aging [26], we suggested that the amino-terminal absence of this unnamed protein might affect its ability of Ca^{2+} binding and modulation in neurons of SAMP8 mice. Several other unidentified protein spots (spots 293, 316, 915, and 1475) which disappeared or uniquely appeared in SAMP8 mice in our study might be also important for understanding the genetic changes.

The second group of differentially expressed proteins included NDRG2, enolase 2, Cu/Zn SOD, myosin, and two unnamed protein products (gi|74214304 and gi|74178239), which changed in an age-related manner, but not strain-related

manner. Among these proteins, NDRG2, enolase 2 and Cu/Zn SOD were already known to be implicated in AD and neurodegeneration. NDRG2 belongs to the N-myc downstream-regulated gene family and is regulated by Myc in human [27]. Both mRNA and protein levels of NDRG2 were markedly increased in the late-onset AD brains, and localized to senile plaques and NFT [28]. Further investigation suggested that NDRG2 was involved in p53-mediated apoptosis [29]. Therefore, the up-regulation of NDRG2 with age in SAM mice might be related to neuron apoptosis during the aging process, since the important role of p53 in neuron apoptosis has been established [30]. Enolase 2, also named neuron-specific enolases (NSE), was down-regulated in the cortex of SAM mice with age. It is a key enzyme in glycolytic pathway, which interconverts 2-phosphoglycerate and phosphoenolpyruvate [31]. NSE was decreased, and significantly oxidized with reduced enzyme activities in the brains of AD patients, which might implicate the metabolic deficits observed in AD [32–34]. Cu/Zn SOD was significantly down-regulated with age in the hippocampus and cortex of both SAM strains. Oxygen radicals are produced as byproducts of normal oxidative metabolism *in vivo*. SOD is an important antioxidant enzyme that protects organism from oxidative damages [35]. A significant decrease in SOD activity was observed in the brains of SAMP8 and AβPP transgenic mice, which might contribute to the elevated oxidative stress and the resultant neuronal degeneration [11, 36]. The direct link between SOD and AD pathology was verified that overexpression of SOD decreased hippocampal superoxide, prevented learning and memory deficits, and reduced Aβ plaques in Tg2576 mouse model of AD [37]. Combination of previous researches and our results of these differential proteins might give important clues for further investigation, which would determine the validity of these proteins as aging-related biomarkers and useful targets for effective diagnosis and therapy.

Except NDRG2, enolase 2 and SOD, myosin, and two unnamed protein products (gi|74214304 and gi|74178239) in the second group were new aging-related proteins, which were never previously reported to be implicated in brain aging or neurodegenerative diseases. Myosins are a large family of structurally diverse molecular motors. Nonmuscle myosin II represents one of the major contributors to the cytoskeleton of neuronal cells [38] and is involved in several functional activities, including cell adhesion, migration, neuritic outgrowth, and possible transport of cellular cargo along the actin cytoskeleton [39–41]. Myosin II-B is the predominant myosin II isoform in neurons. Downregulation of myosin II-B by siRNA altered the subcellular localization of the AβPP and increased Aβ deposition in N2a cells [42]. Thus, the upregulation of myosin with age might be a compensatory response to the aging-related increase of Aβ deposition in the cortex of SAMP8 mice. However, the mechanisms remain to be investigated. For the two unnamed protein products (gi|74214304 and gi|74178239), we performed database mining (http://hits.isb-sib.ch/cgi-bin/PFSCAN). The results showed that these two unnamed protein products putatively had many casein kinase II phosphorylation sites and protein kinase C phosphorylation sites, indicating that they might be signal transducers. Further investigation in their physiological and pathological functions will provide important information for the pathogenesis of brain aging.

The third group of differentially expressed protein was heme binding protein 1, which specifically changed in the hippocampus of SAMP8 with age-related manner. Heme serves as the prosthetic group of numerous hemoproteins (e.g., hemoglobin, myoglobin, cytochromes, guanylate cyclase, and nitric oxide synthase) and plays an important role in many physiological functions. However, free heme is a prooxidant and has high affinity for different cell structures (protein, membranes, and DNA), triggers site-directed oxidative damage [43]. Evidences showed that toxic free heme was increased in the aged or AD brain, which resulted in mitochondrial decay, oxidative stress, and iron accumulation [44, 45]. Heme binding protein 1 belongs to heme detoxification systems, and detoxifies free heme by forming a non-toxic hemecomplex [43]. In the present study, we reported the downregulation of heme binding protein 1 in the aged brain for the first time, and speculated that this might contribute to the abnormal metabolism of heme and eventually lead to the pathologically accelerated aging of SAMP8 mice.

In conclusion, our present study identified three groups of differentially expressed proteins in SAMP8 and SAMR1 mice by using comparative proteomics. The first group contained SAMP8-specific differential proteins including Uchl3, mitofilin, AK4, and an unnamed protein product (gi|12847201). They might be implicated in the genetic difference between SAMP8 and SAMR1 mice. The second group contained the age-related differential proteins, which were particularly interesting since they were associated with brain aging. It included NDRG2, enolase 2, Cu/Zn SOD, myosin and two unnamed protein products

(gi|74214304 and gi|74178239). The third group was SAMP8-specific and age-related proteins that contained heme binding protein 1. In addition, we found 5 spots that could not be identified based on the present condition of MS analysis. Spots 293, 316, 915, and 1475 belonged to the first group, and spot 2440 belonged to the second group. These unidentified differential spots might be new proteins that have never been reported, particularly expressed differentially in SAMP8 mice and in the aged brain. They were therefore valuable for further study. Our finding provides new information for investigating the pathogenesis of brain aging. Some of these proteins might be used as age-related biomarkers and targets for diagnosis and therapy.

ACKNOWLEDGMENTS

This work was supported by the grant from the Ministry of Education, China. No. IRT0514; and Major Scientific and Technological Special Project from the Ministry of Science and Technology, No. 2009ZX09303-003.

Authors' disclosures available online (http://www.j-alz.com/disclosures/view.php?id=656).

REFERENCES

[1] Keller JN (2006) Age-related neuropathology, cognitive decline and Alzheimer's disease. *Ageing Res Rev* **5**, 1-13.

[2] Morrison JH, Hof PR (1997) Life and death of neurons in the aging brain. *Science* **278**, 412-419.

[3] Esiri MM (2007) Ageing and the brain. *J Pathol* **211**, 181-187.

[4] Yankner BA, Lu T, Loerch P (2008) The aging brain. *Annu Rev Pathol* **3**, 41-66.

[5] Xiong J, Camello PJ, Verkhratsky A, Toescu EC (2004) Mitochondrial polarisation status and $[Ca^{2+}]i$ signalling in rat cerebellar granule neurones aged *in vitro*. *Neurobiol Aging* **25**, 349-359.

[6] Head E (2009) Oxidative damage and cognitive dysfunction-antioxidant treatments to promote healthy brain aging. *Neurochem Res* **34**, 670-678.

[7] Takeda T, Hosokawa M, Takeshita S, Irino M, Higuchi K, Matsushita T, Tomita Y, Yasuhira K, Hamamoto H, Shimizu K, Ishii M, Yamamuro T (1981) A new murine model of accelerated senescence. *Mech Ageing Dev* **17**, 183-194.

[8] Takeda T (1999) Senescence-accelerated mouse (SAM): a biogerontological resource in aging research. *Neurobiol Aging* **20**, 105-110.

[9] Watanabe K, Tonosaki K, Kawase T, Karasawa N, Nagatsu I, Fujita M, Onozuka M (2001) Evidence for involvement of dysfunctional teeth in the senile process in the hippocampus of SAMP8 mice. *Exp Gerontol* **36**, 283-295.

[10] Pallas M, Camins A, Smith MA, Perry G, Lee HG, Casadesus G (2008) From aging to Alzheimer's disease: unveiling "the switch" with the senescence-accelerated mouse model (SAMP8). *J Alzheimers Dis* **15**, 615-624.

[11] Alvarez-García O, Vega-Naredo I, Sierra V, Caballero B, Tomás-Zapico C, Camins A, García JJ, Pallàs M, Coto-Montes A (2006) Elevated oxidative stress in the brain of senescence-accelerated mice at 5 months of age. *Biogerontology* **7**, 43-52.

[12] Sureda FX, Gutierrez-Cuesta J, Romeu M, Mulero M, Canudas AM, Camins A, Mallol J, Pallàs M (2006) Changes in oxidative stress parameters and neurodegeneration markers in the brain of the senescence-accelerated mice SAMP-8. *Exp Gerontol* **41**, 360-367.

[13] Takemura M, Nakamura S, Akiguchi I, Ueno M, Oka N, Ishikawa S, Shimada A, Kimura J, Takeda T (1993) Beta/A4 proteinlike immunoreactive granular structures in the brain of senescence-accelerated mouse. *Am J Pathol* **142**, 1887-1897.

[14] Morley JE, Kumar VB, Bernardo AE, Farr SA, Uezu A, Tumosa N, Flood JF (2000) Beta-amyloid precursor polypeptide in SAMP8 mice affects learning and memory. *Peptides* **21**, 1761-1767.

[15] Tomobe K, Nomura Y (2009) Neurochemistry, neuropathology, and heredity in SAMP8: a mouse model of senescence. *Neurochem Res* **34**, 660-669.

[16] Pandey A, Mann M (2000) Proteomics to study genes and genomes. *Nature* **405**, 837-846.

[17] Poon HF, Castegna A, Farr SA, Thongboonkerd V, Lynn BC, Banks WA, Morley JE, Klein JB, Butterfield DA (2004) Quantitative proteomics analysis of specific protein expression and oxidative modification in aged senescence-accelerated-prone 8 mice brain. *Neuroscience* **126**, 915-926.

[18] Wang Q, Liu Y, Zou X, Wang Q, An M, Guan X, He J, Tong Y, Ji J (2008) The hippocampal proteomic analysis of senescence-accelerated mouse: implications of Uchl3 and mitofilin in cognitive disorder and mitochondria dysfunction in SAMP8. *Neurochem Res* **33**, 1776-1782.

[19] Candiano G, Bruschi M, Musante L, Santucci L, Ghiggeri GM, Carnemolla B, Orecchia P, Zardi L, Righetti PG (2004) Blue silver: a very sensitive colloidal Coomassie G-250 staining for proteome analysis. *Electrophoresis* **25**, 1327-1333.

[20] Díez-Vives C, Gay M, García-Matas S, Comellas F, Carrascal M, Abian J, Ortega-Aznar A, Cristòfol R, Sanfeliu C (2009) Proteomic study of neuron and astrocyte cultures from senescence-accelerated mouse SAMP8 reveals degenerative changes. *J Neurochem* **111**, 945-955.

[21] Goldberg AL (2003) Protein degradation and protection against misfolded or damaged proteins. *Nature* **426**, 895-899.

[22] John GB, Shang Y, Li L, Renken C, Mannella CA, Selker JM, Rangell L, Bennett MJ, Zha J (2005) The mitochondrial inner membrane protein mitofilin controls cristae morphology. *Mol Biol Cell* **16**, 1543-1554.

[23] Tomasselli AG, Noda LH (1979) Mitochondrial GTP-AMP phosphotransferase. 2. Kinetic and equilibrium dialysis studies. *Eur J Biochem* **93**, 263-267.

[24] Liu R, Ström AL, Zhai J, Gal J, Bao S, Gong W, Zhu H (2009) Enzymatically inactive adenylate kinase 4 interacts with mitochondrial ADP/ATP translocase. *Int J Biochem Cell Biol* **41**, 1371-1380.

[25] Melkonian KA, Ostermeyer AG, Chen JZ, Roth MG, Brown DA (1999) Role of lipid modifications in targeting proteins to detergent-resistant membrane rafts. Many raft proteins are acylated, while few are prenylated. *J Biol Chem* **274**, 3910-3917.

[26] Raza M, Deshpande LS, Blair RE, Carter DS, Sombati S, DeLorenzo RJ (2007) Aging is associated with elevated

intracellular calcium levels and altered calcium homeostatic mechanisms in hippocampal neurons. *Neurosci Lett* **418**, 77-81.

[27] Zhang J, Li F, Liu X, Shen L, Liu J, Su J, Zhang W, Deng Y, Wang L, Liu N, Han W, Zhang J, Ji S, Yang A, Han H, Yao L (2006) The repression of human differentiation-related gene NDRG2 expression by Myc via Miz-1-dependent interaction with the NDRG2 core promoter. *J Biol Chem* **281**, 39159-39168.

[28] Mitchelmore C, Büchmann-Møller S, Rask L, West MJ, Troncoso JC, Jensen NA (2004) NDRG2: a novel Alzheimer's disease associated protein. *Neurobiol Dis* **16**, 48-58.

[29] Liu N, Wang L, Li X, Yang Q, Liu X, Zhang J, Zhang J, Wu Y, Ji S, Zhang Y, Yang A, Han H, Yao L (2008) N-Myc downstream-regulated gene 2 is involved in p53-mediated apoptosis. *Nucleic Acids Res* **36**, 5335-5349.

[30] Jordán J, Galindo MF, Prehn JH, Weichselbaum RR, Beckett M, Ghadge GD, Roos RP, Leiden JM, Miller RJ (1997) p53 expression induces apoptosis in hippocampal pyramidal neuron cultures. *J Neurosci* **17**, 397-405.

[31] Trapp BD, Marangos PJ, Webster HD (1981) Immunocytochemical localization and developmental profile of neuron specific enolase (NSE) and non-neuronal enolase (NNE) in aggregating cell cultures of fetal rat brain. *Brain Res* **220**, 121-130.

[32] Kato K, Kurobe N, Suzuki F, Morishita R, Asano T, Sato T, Inagaki T (1991) Concentrations of several proteins characteristic of nervous tissue in cerebral cortex of patients with Alzheimer's disease. *J Mol Neurosci* **3**, 95-99.

[33] Butterfield DA, Gnjec A, Poon HF, Castegna A, Pierce WM, Klein JB, Martins RN (2006) Redox proteomics identification of oxidatively modified brain proteins in inherited Alzheimer's disease: an initial assessment. *J Alzheimers Dis* **10**, 391-397.

[34] Sultana R, Boyd-Kimball D, Poon HF, Cai J, Pierce WM, Klein JB, Merchant M, Markesbery WR, Butterfield DA (2006) Redox proteomics identification of oxidized proteins in Alzheimer's disease hippocampus and cerebellum: an approach to understand pathological and biochemical alterations in AD. *Neurobiol Aging* **27**, 1564-1576.

[35] Shi Q, Gibson GE (2007) Oxidative stress and transcriptional regulation in Alzheimer disease. *Alzheimer Dis Assoc Disord* **21**, 276-291.

[36] Schuessel K, Schäfer S, Bayer TA, Czech C, Pradier L, Müller-Spahn F, Müller WE, Eckert A (2005) Impaired Cu/Zn-SOD activity contributes to increased oxidative damage in APP transgenic mice. *Neurobiol Dis* **18**, 89-99.

[37] Massaad CA, Washington TM, Pautler RG, Klann E (2009) Overexpression of SOD-2 reduces hippocampal superoxide and prevents memory deficits in a mouse model of Alzheimer's disease. *Proc Natl Acad Sci U S A* **106**, 13576-13581.

[38] Rochlin MW, Itoh K, Adelstein RS, Bridgman PC (1995) Localization of myosin II A and B isoforms in cultured neurons. *J Cell Sci* **108**, 3661-3670.

[39] Conti MA, Even-Ram S, Liu C, Yamada KM, Adelstein RS (2004) Defects in cell adhesion and the visceral endoderm following ablation of nonmuscle myosin heavy chain II-A in mice. *J Biol Chem* **279**, 41263-41266.

[40] Ma X, Kawamoto S, Hara Y, Adelstein RS (2004) A point mutation in the motor domain of nonmuscle myosin II-B impairs migration of distinct groups of neurons. *Mol Biol Cell* **15**, 2568-2579.

[41] Turney SG, Bridgman PC (2005) Laminin stimulates and guides axonal outgrowth via growth cone myosin II activity. *Nat Neurosci* **8**, 717-719.

[42] Massone S, Argellati F, Passalacqua M, Armirotti A, Melone L, d'Abramo C, Marinari UM, Domenicotti C, Pronzato MA, Ricciarelli R (2007) Downregulation of myosin II-B by siRNA alters the subcellular localization of the amyloid precursor protein and increases amyloid-beta deposition in N2a cells. *Biochem Biophys Res Commun* **362**, 633-638.

[43] Kumar S, Bandyopadhyay U (2005) Free heme toxicity and its detoxification systems in human. *Toxicol Lett* **157**, 175-188.

[44] Bitar MS, Shapiro BH (1987) Aberration of heme and hemoprotein in aged female rats. *Mech Ageing Dev* **38**, 189-197.

[45] Smith MA, Nunomura A, Zhu X, Takeda A, Perry G (2000) Metabolic, metallic, and mitotic sources of oxidative stress in Alzheimer disease. *Antioxid Redox Signal* **2**, 413-420.